

# Evidence for a high-density amorphous form in indomethacin from Raman scattering investigations

Alain Hédoux,<sup>1</sup> Yannick Guinet,<sup>1</sup> Frédéric Capet,<sup>2</sup> Laurent Paccou,<sup>1</sup> and Marc Descamps<sup>1</sup>

<sup>1</sup>*Laboratoire de Dynamique et Structure des Matériaux Moléculaires, UMR CNRS 8024, Université des Sciences et Technologies de Lille, UFR de Physique, Bâtiment P5, 59655 Villeneuve d'Ascq Cédex, France*

<sup>2</sup>*Unité de Catalyse et Chimie du Solide, UMR CNRS 8181, Université des Sciences et Technologies de Lille, 59655 Villeneuve d'Ascq Cédex, France*

(Received 7 November 2007; revised manuscript received 28 February 2008; published 28 March 2008)

Pressure-induced transformation of  $\gamma$ -IMC [1-(*p*-chlorobenzoyl)-5-methoxy-2-methylindole-3-acetic acid] is analyzed from Raman scattering investigations in the low-frequency range of 10–250 cm<sup>-1</sup> and the high frequency region between 1550 and 1750 cm<sup>-1</sup>, where C=O stretching vibrations are usually observed. At room temperature, by pressurization from atmospheric pressure up to 4 GPa,  $\gamma$ -IMC undergoes a collapse transformation into a high-pressure crystalline form, induced by large rearrangement in the hydrogen-bonded network associated with molecular conformational changes. The Raman spectrum of the high-pressure crystal is similar to that of the  $\alpha$  form, which is denser than the  $\gamma$  form and metastable with respect to  $\gamma$ -IMC at atmospheric pressure. Upon further compression a solid-state amorphization is observed via the breakdown of hydrogen bonds. The Raman line shape of the high-pressure amorphous form is different from that of the vitreous state (or thermal glass obtained by quenching the liquid), suggesting the existence of a high-density amorphous state. By release of pressure, this high-density amorphous state transforms into the thermal glass. This transformation can be interpreted as a transformation between a high-density amorphous to a low-density amorphous state, which could be associated with a polyamorphic transformation.

DOI: 10.1103/PhysRevB.77.094205

PACS number(s): 78.30.Ly, 61.43.-j, 62.50.-p, 64.70.K-

## I. INTRODUCTION

In the past decade, polyamorphism has focused considerable theoretical and experimental investigations. Polyamorphism refers to the existence of two different amorphous states of the same substance, which is linked via a first-order phase transition. The study of polyamorphic transitions has been enabled by the development of diamond anvil cells, giving the opportunity of current investigations in the range of several 10 GPa since most of these transitions can be observed under very high pressures. In some cases, discontinuous structural changes on densification have been detected and characterized as first-order phase transformations. Ice is one of the most currently example used to illustrate polyamorphic transitions. The structural changes between the low- and the high-density amorphous state transitions have been evidenced from x-ray<sup>1</sup> and neutron diffraction experiments.<sup>1</sup> Pressure-induced amorphization (PIA) was also reported for H<sub>2</sub>O from pressurization of hexagonal ice (Ih).<sup>2,3</sup> The amorphous ice obtained by compression of hexagonal ice and named high-density amorphous (HDA) is structurally distinct from the low-density amorphous state (LDA) obtained by condensation from vapor. In this context, PIA can be considered as a tool to investigate polyamorphism situations. Another polyamorphic transition, which is similar to the HDA-LDA transition, is also expected between tetrahedrally coordinated forms of  $\alpha$ -SiO<sub>2</sub>,<sup>4,5</sup> GeO<sub>2</sub>,<sup>6,7</sup> and structural changes detected in liquid phosphorus<sup>8</sup> or liquid GeSe<sub>2</sub> (Refs. 9 and 10) are highly suggestive of a liquid-liquid first-order transition. However, despite the observation of PIA in some molecular systems,<sup>11–17</sup> no polyamorphic transition was yet detected in organic molecular compounds, except the controversial case of triphenyl phosphite.<sup>18–25</sup>

Indomethacin (IMC) [1-(*p*-chlorobenzoyl)-5-methoxy-2-methylindole-3-acetic acid] [Fig. 1(a)] is an anti-inflammatory, antipyretic, and analgesic drug, which exhibits a rich and very original polymorphism that is characterized by the  $\alpha$ - $\gamma$  monotropic system, whose the more stable form is the  $\gamma$  phase.<sup>26</sup> Moreover, the more stable phase does not exhibit the highest density with respect to other crystalline states. The  $\gamma$  phase which melts at  $T_m=434$  K.<sup>27</sup> Crystal of  $\gamma$ -IMC belongs to the centrosymmetric triclinic space group  $P\bar{1}$  with  $Z=2$ .<sup>28</sup> The crystal packing is characterized by molecular associations in dimmers [Fig. 1(b)] via hydrogen bonding of the carboxylic acid group. The metastable  $\alpha$  phase, which is obtained by dissolution in methanol and precipitation in water,<sup>29</sup> crystallizes in the  $P2_1$  space group ( $Z=6$ ) (Ref. 30) and melts at 428 K.<sup>27</sup> The organization in trimers of the  $\alpha$  phase [Fig. 1(c)] is suspected to be at the origin of its higher density<sup>30</sup> (1.40) with respect to that of the stable  $\gamma$  phase (1.38). The  $\delta$  form is obtained by isothermal aging of the supercooled liquid at 353 K, which is in agreement with Borka.<sup>31</sup> The  $\delta$  IMC structure was not solved and no information about molecular association via hydrogen bond was reported.

In a recent study,<sup>32</sup> PIA of IMC was suggested from the observation of the broadening of Bragg peaks, without obtaining a completely amorphous state. Consequently, this paper focuses on Raman investigations of pressurized  $\gamma$ -IMC in order to analyze pressure-induced transformations of  $\gamma$ -IMC and principally pressure-induced disordering toward amorphous state in an original polymorphic molecular system. The capability of IMC to be candidate polyamorphic system, i.e., to undergo a first-order amorphous-amorphous transition, is analyzed. Special attention is given to the analysis of the stability of the hydrogen-bond network on pressur-

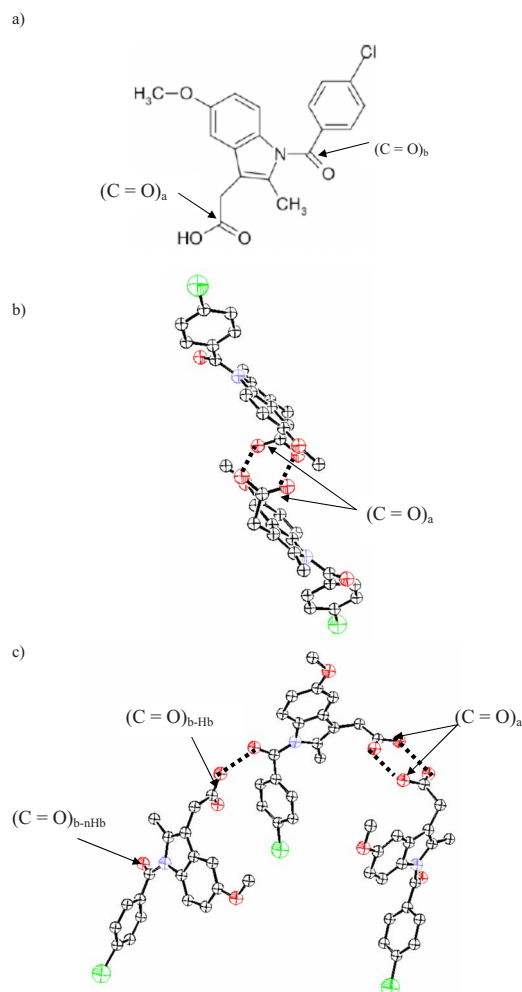


FIG. 1. (Color online) Representation of the (a) IMC molecule and molecular associations (b) in dimmers distinctive of the  $\gamma$  form and (c) in trimmers distinctive of the  $\alpha$  form. The different kinds of C=O stretching bands are associated with the C=O bonds by arrows.

ization and its influence on the mechanism of pressure-induced amorphization.

IMC appears as an interesting system for Raman investigations on polymorphic transformations, and also to analyze the molecular packing via hydrogen bonds (H bonds) and PIA mechanism since the different crystalline forms and the amorphous state can be characterized in the 1550–1750  $\text{cm}^{-1}$  frequency range.<sup>33,34</sup> In this frequency range, C=O stretching vibrations involved in molecular associations via H bonds are Raman active.<sup>34,35</sup>

## II. MATERIALS AND METHODS

The  $\gamma$  form of indomethacin ( $\gamma$ -IMC) with a purity of 99% is supplied from FLUKA and used as received. Experiments were performed at room temperature on powder of  $\gamma$  IMC.

Pressure was generated in a gasketed membrane diamond anvil cell. Measurements were carried out without any pres-

sure transmitting medium. Sample size was typically 210  $\mu\text{m}$  diameter and 110  $\mu\text{m}$  thickness. Three ruby crystals (size of  $\sim 10 \mu\text{m}$ ) were included for *in situ* pressure measurements by the standard ruby fluorescence technique<sup>36</sup> with an accuracy of  $\pm 0.1$  GPa. Two pressure runs were done in the 0–14 GPa pressure range. The first one was carried out in 2 days with pressure increasing by regular steps of about 0.5 GPa. Pressure was then slowly released by step of 1 GPa. Rapid pressurization of  $\gamma$ -IMC was performed with larger pressure steps to reach 14 GPa in 2 hours. Raman spectra recorded in the two different runs were observed to be similar at comparable pressure. Only the results obtained in the slowest pressurization are reported in this paper. Pressure measurements on the three ruby crystals indicate that pressure gradients in the sample were insignificant over the studied range of 0–10 GPa.

The backscattering spectra were recorded in the low-frequency range of 10 and 250  $\text{cm}^{-1}$  and in the 1550–1750  $\text{cm}^{-1}$  frequency range using a DILOR-XY spectrometer equipped with a liquid nitrogen cooled charge coupled device detector. Spectrometer slits were kept at 300  $\mu\text{m}$  which give a resolution-limited width of 2  $\text{cm}^{-1}$  in the high frequency region. The 647.1 nm line of a mixed argon-krypton laser was used for Raman excitation. An Olympus 50 $\times$  long-working distance objective was used. The volume analyzed by microspectroscopy using a confocal hole of 600  $\mu\text{m}$  was about 300  $\mu\text{m}^3$ .

Frequencies in the low- and high-frequency Raman spectra were determined using the residue method in the fitting procedure of the PEAKFIT software (Jandel Scientific Software).

## III. RESULTS

### A. Raman spectra of different states of indomethacin

The low-frequency Raman spectra of amorphous and crystalline states are plotted in Fig. 2. Low-frequency Raman spectra of crystalline states are composed of phonon peaks corresponding to the lattice vibrations and then reflecting the long-range order in crystals. The low-frequency Raman spectrum is distinctive of each crystalline form, and the number of Raman active phonons is directly dependent on the degree of symmetry of the crystal. It is clearly observed in Fig. 2 that the degree of symmetry of the metastable  $\alpha$  form is lower than that of  $\gamma$ -IMC. By contrast to the crystalline states, no phonon peak is observed in the amorphous state since there is no long-range order. The low-frequency spectrum of vitreous IMC (thermal glass) is only composed of a broadband directly related to the vibrational density of states distinctive of the short-range order and mainly resulting from an inhomogeneous broadening of phonon peaks.

The Raman spectra of the amorphous solid and crystalline states in the 1550–1750  $\text{cm}^{-1}$  range are plotted in Fig. 3. In this region, C=O stretching ( $\nu\text{C=O}$ ) bands are typically observed<sup>34,35,37</sup> between 1600 and 1750  $\text{cm}^{-1}$ .

The assignment of Raman bands observed in this region is reported in Table I from previous studies.<sup>34,35</sup> This frequency range was previously determined as very sensitive to molecular associations via hydrogen bonding.<sup>34,38,39</sup> Amorphous

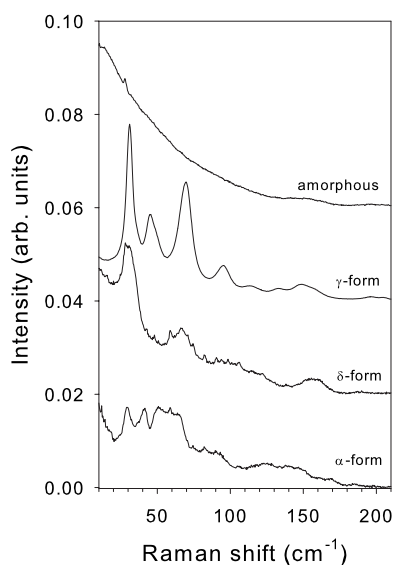


FIG. 2. The low-frequency Raman spectra of crystalline forms and the amorphous state at room temperature conditions.

IMC is considered as mainly composed of cyclic dimmers with a too small proportion of H-bonded molecules to form a chain,<sup>34</sup> whereas the structure of the  $\gamma$  form is organized in chains of dimmers. No Raman band in the C=O stretching region is directly informative of molecular associations via H bonds between acid groups, both in amorphous state and in the  $\gamma$  form.<sup>34</sup> However, the 1679 and 1697  $\text{cm}^{-1}$  bands detected, respectively, in the amorphous state and in the  $\gamma$  form and both assigned to the benzoyl C=O stretching vibration [ $\nu(\text{C}=\text{O})_b$ ] exhibits a contrasted line shape depending on the organization of IMC molecules. In the  $\gamma$  form, the 1697  $\text{cm}^{-1}$  band is influenced by steric hindrance and tension of molecules<sup>35</sup> imposed by H-bonded associations in dim-

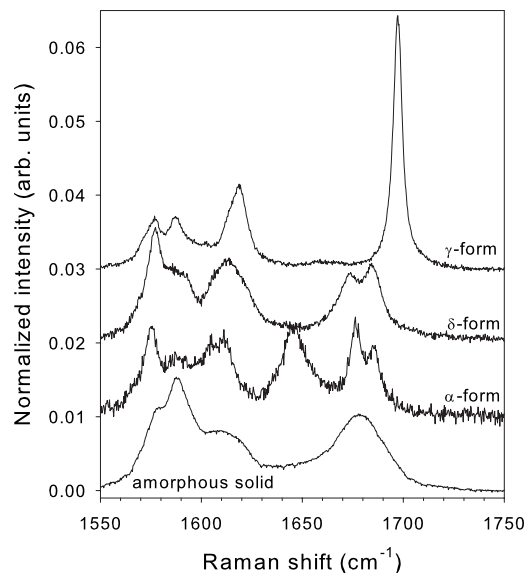


FIG. 3. Raman spectra in the C=O stretching region for indomethacin polymorphs and the solid amorphous state under room temperature conditions.

TABLE I. Assignment of Raman bands in the 1600–1750  $\text{cm}^{-1}$  region.

Raman band ( $\text{cm}^{-1}$ )	Form	Assignment
1588	$\gamma$	Ring vibration of indole
1589	Amorphous, $\delta$	
1591	$\alpha$	
1611	Amorphous, $\alpha$	$\nu\text{C}=\text{C}$
1614	$\delta$	
1618	$\gamma$	
1648	$\alpha$	H-bonded acid $\nu(\text{C}=\text{O})_a$
1673	$\delta$	H-bonded benzoyl $\nu(\text{C}=\text{O})_{b-\text{Hb}}$
1678	$\alpha$	
1679	Amorphous	(Non-H bonded+H bonded) benzoyl $\nu(\text{C}=\text{O})_b$
1685	$\delta$	Non-H bonded benzoyl $\nu(\text{C}=\text{O})_{b-\text{nHb}}$
1688	$\alpha$	
1697	$\gamma$	Benzoyl $\nu(\text{C}=\text{O})_b$

mers. Consequently, the frequency and the sharpness of this band reflect the long-range order of dimer chains. This band is distinctive of the  $\gamma$  form, and its width can be used to probe and to monitor the long-range order in the  $\gamma$  form. By contrast, the broadened line shape of the 1679  $\text{cm}^{-1}$  band in the amorphous state (Fig. 3) is probably inherent to the local disorder or to the presence of different molecular conformations, as it was determined in the  $\alpha$  form.<sup>30</sup> The spectrum of  $\alpha$ -IMC is more complex in this region. It is the consequence of the presence of three different molecular conformations and additional H bonding. The Raman bands at 1648 and 1678  $\text{cm}^{-1}$  have been previously assigned to H bonded acid C=O stretch<sup>34</sup> [ $\nu(\text{C}=\text{O})_a$ ]. These bands would be Raman active because of the presence of three different molecular conformations in the  $\alpha$  form. By taking into account the assignment of the 1697  $\text{cm}^{-1}$  band in the  $\gamma$  form and the 1679  $\text{cm}^{-1}$  band in the amorphous state the 1678 and 1688  $\text{cm}^{-1}$  doublet should be assigned, respectively, to the H bonded and non-H bonded benzoyl C=O stretching bands since there are probably two different frequencies corresponding to the C=O stretch of benzoyl groups involved in molecular associations via H bonds with acid groups and to C=O stretch for free benzoyl groups. The Raman band at 1648  $\text{cm}^{-1}$  is assigned to the C=O stretching vibration of hydrogen bonded acid, which is in agreement with previous studies.<sup>34,35</sup> As a consequence of this new assignment, the broadband observed at 1679  $\text{cm}^{-1}$  in the amorphous state which appears as the envelope of the 1678 and 1688  $\text{cm}^{-1}$  can be interpreted as corresponding to both types (H bonded and non-H bonded) of benzoyl C=O stretching vibrations, as suggested by Schmidt *et al.*<sup>35</sup> The tail observed on its low-frequency side overlap on the frequency range of the 1648  $\text{cm}^{-1}$  band which is characteristic of trimmer associa-

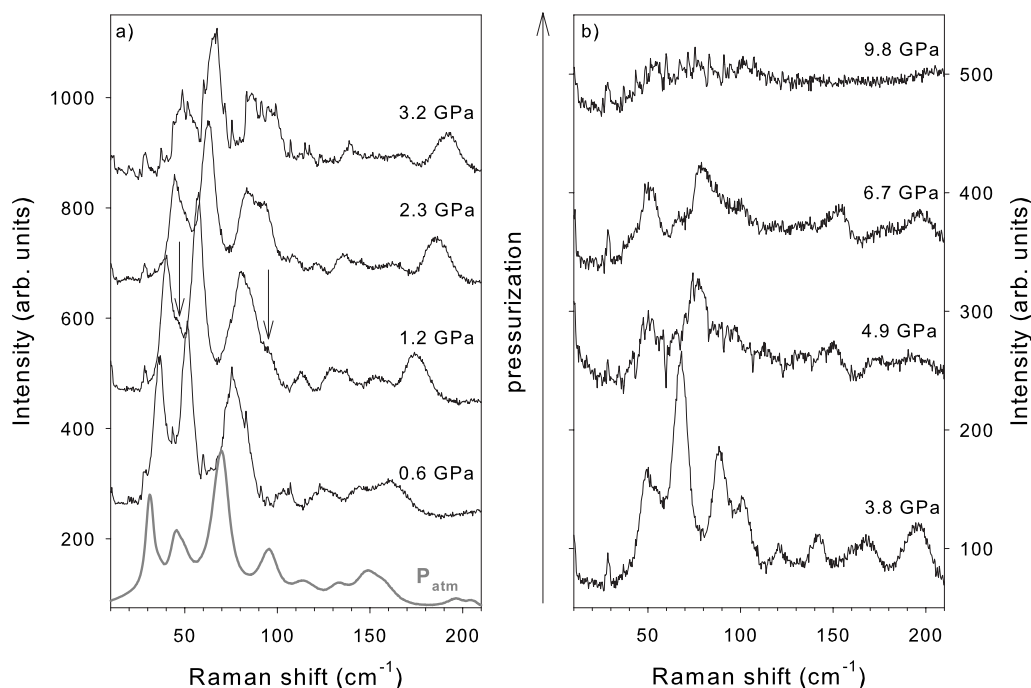


FIG. 4. Pressure dependence of the low-frequency Raman spectrum on pressurization.

tions in the  $\alpha$  form. In this context, it can be assumed that the broadband centered around  $1697\text{ cm}^{-1}$  corresponds to an homogenous distribution of  $\text{C}=\text{O}$  stretching frequencies, indicating the existence of molecular associations via H bonding detected in the different crystalline forms, with probably a maximum of intensity corresponding to no molecular association. There is no structural information on the  $\delta$  phase reported in the literature. The Raman bands detected in the  $1670\text{--}1685\text{ cm}^{-1}$  range (Fig. 3) can be tentatively assigned, as in the  $\alpha$  form (Table I), to H and non-H bonded benzoyl  $\text{C}=\text{O}$  stretching vibrations. This could also indicate the existence of different molecular conformations in the  $\delta$  form. However, the present study indicates that molecular associations in the  $\delta$  form should be different from trimers observed in the  $\alpha$  form since no Raman is observed around  $1648\text{ cm}^{-1}$ .

### B. Pressure dependence of the Raman spectrum on pressurization

In the low-frequency range (LFRS), the pressure dependence of the Raman spectrum of IMC pressurized from the  $\gamma$  form is plotted in Fig. 4. A strong pressure dependence of the LFRS is observed between  $P_{\text{atm}}$  and 0.6 GPa. Phonon peaks are shifted toward high frequencies, and the lattice mode near  $50\text{ cm}^{-1}$  exhibits a clear intensity increase with a concomitant sharpening. Above 0.6 GPa, two additional phonon peaks are detected (localized by arrows in Fig. 4). These observations could be associated with a distortion of the lattice of  $\gamma$ -IMC. Above 3.8 GPa, a change in the Raman line shape is clearly detected. It is indicative of changes in the long-range order, i.e., a crystal-crystal transition. The spectral modifications observed in the low-frequency range between atmospheric pressure and 3.8 GPa (Fig. 4) can be as-

sociated with an ordering process. By taking into account the weak intensity and the poor quality of the Raman spectrum at 4.9 GPa and above, the crystalline state above 3.8 GPa cannot be identified. However, it can be observed that the most intense phonon peak in the spectrum recorded at 3.8 GPa strongly decreases and broadens, as well as both modes, at frequencies just higher than the latter, which are merging. The line shape of the LFRS of the pressurized  $\gamma$  form becomes resembling that of the  $\alpha$  form. With further pressurization above 6.7 GPa, the spectrum flattens and mimics the spectrum of an amorphous state, despite the very low quality of this spectrum which is perturbed by rotational bands of diatomic molecules ( $\text{N}_2$ ,  $\text{O}_2$ , etc.) in the air.

The pressure dependence of the Raman spectrum between  $1550$  and  $1750\text{ cm}^{-1}$  is shown in Figs. 5(a) and 5(b). The pressure dependence of the spectrum recorded in the  $1550\text{--}1750\text{ cm}^{-1}$  is dominated by the original behavior of the  $1697\text{ cm}^{-1}$  band on pressurization compared to other bands in the  $1550\text{--}1750\text{ cm}^{-1}$  region. This band exhibits no significant frequency shift up to 3.2 GPa contrasting strongly with the other bands in the spectrum. By pressurization from atmospheric pressure, a Raman band around  $1615\text{ cm}^{-1}$  is gradually growing in the low-frequency side of the Raman band assigned to the  $\text{C}=\text{C}$  stretching vibration (Table I). It is worth noting that a doublet is observed in the Raman spectrum of the  $\alpha$  form in the  $\text{C}=\text{C}$  stretching region (Fig. 3, and Table I). The gradual growth of this band indicates probably a progressive conformational change of IMC toward molecular conformations distinctive of the  $\alpha$  phase. The observation of this additional band in the  $1550\text{--}1750\text{ cm}^{-1}$  region can be considered as accompanying spectral changes in the low-frequency range and so confirms the interpretation of pressure-induced ordering process. Above 3.2 GPa, a Raman band is slowly growing under



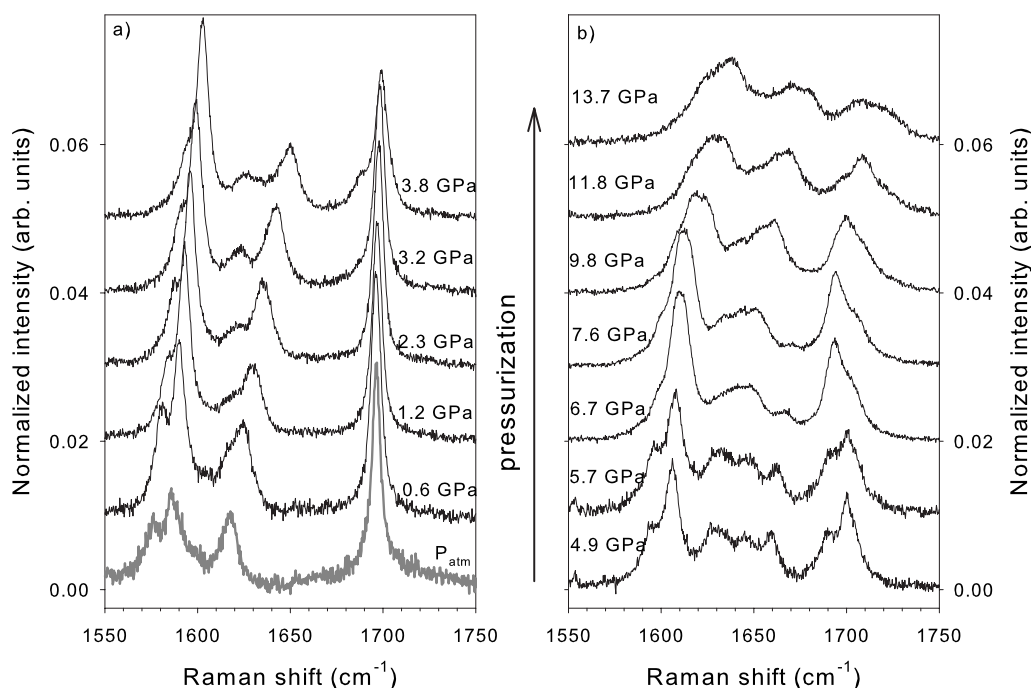


FIG. 5. Pressure dependence of the Raman spectrum in the 1550–1750  $\text{cm}^{-1}$  region on pressurization.

pressurization in the low-frequency side of the 1697  $\text{cm}^{-1}$  band. It is clearly observed in Fig. 5(b) that the intensity of the growing band increases to the detriment of the 1697  $\text{cm}^{-1}$  band which exhibits a concomitant intensity decrease. This behavior indicates that the organization in chains of dimmers is disrupted and a new organization, which is similar to that in the  $\alpha$  or  $\delta$  forms, develops. Above 3.2 GPa, it can be also noticed that the 1697  $\text{cm}^{-1}$  band significantly shifts and broadens with pressurization. At 4.9 GPa, two bands are clearly detected around 1700  $\text{cm}^{-1}$  which can be associated with the bands assigned to H bonded and non-H bonded benzoyl C=O stretching vibration in the  $\alpha$  and  $\delta$  crystalline forms. Between 1650 and 1675  $\text{cm}^{-1}$ , one additional band is detected, probably representative of the appearance of molecular associations different from dimmers. By further pressurizing, this band disappears and the spectrum becomes mainly composed of three broad bands, suggestive of an amorphous state. Above 4.9 GPa, Fig. 5(b) clearly reveals a pressure-induced disordering process. It can be outlined that the Raman lineshape in this frequency range is not similar to that obtained by vitrification of liquid IMC and so could be considered as characteristic of a high density amorphous state.

### C. Pressure dependence of the Raman spectrum on depressurization

Pressure was slowly released by step of 0.5–1 GPa. By taking into account the poor quality of the LFRS, only the 1550–1750  $\text{cm}^{-1}$  region was analyzed during the release of pressure. The pressure dependence of the spectrum is shown in Fig. 6. From 9 GPa down to 4.6 GPa, the Raman line shape of the spectrum resembles more and more that of the amorphous state obtained by vitrification. This is suggestive

of a transformation of a high density amorphous state into a low-density amorphous state (thermal glass) which is usually obtained by a quench of the liquid state. The opposite transformation (low-to high-density amorphous form) was not distinctively observed by pressurization in Fig. 5. At 4 GPa, two bands are clearly detected around 1700  $\text{cm}^{-1}$ . This observation indicates the formation of molecular associations in dimmers distinctive of the  $\gamma$  crystalline form. Only the high-frequency band remains active by further pressure decreasing. The intensity increase of this band accompanying with a concomitant sharpening indicates the progressive extension of dimmer chains to the detriment of non H-bonded molecules, i.e., the development of the long-range order of the  $\gamma$  form in the matrix of the thermal glass. The Raman spectrum recorded at 1.5 GPa is similar to that of the  $\gamma$  form. By depressurization, the high-density amorphous state transforms into the low-density state structurally similar to the quenched liquid (thermal glass) and previously described as mainly composed of non H-bonded IMC molecules.<sup>34</sup> By further depressurization, the H-bond network in dimmers distinctive of the  $\gamma$  phase is preferentially formed, rather than the close packing in trimmers of the  $\alpha$  phase. Consequently, the synthesis route toward the high-density amorphous state by pressurization is not reversible.

## IV. ANALYSIS OF RAMAN DATA

### A. Analysis of the mechanism of pressure-induced transformations

The analysis of both  $\omega(P)$  curves (Figs. 7 and 8) and  $d\omega/dP$  values (Table II) in the low-frequency and in the 1550–1750  $\text{cm}^{-1}$  regions reveals a drastic difference between the pressure dependence of external and internal

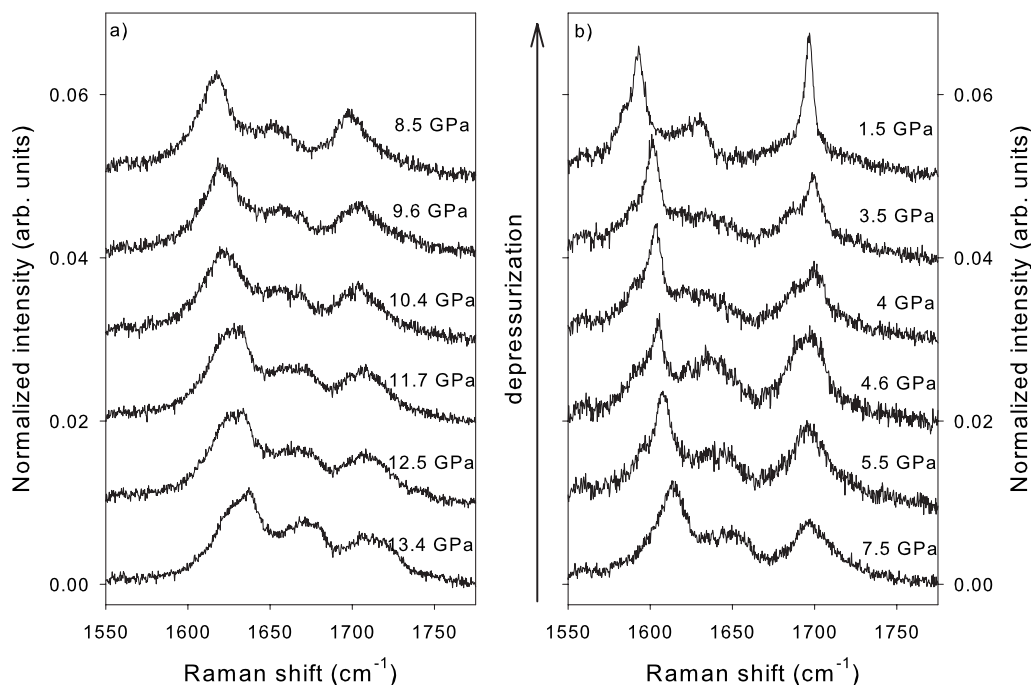


FIG. 6. Pressure dependence of the Raman spectrum in the 1550–1750  $\text{cm}^{-1}$  by release of pressure.

modes below 1 GPa. This strong discrepancy in the behavior of intermolecular and intramolecular vibrations reflects the disparity between the internal and external modes in molecular compounds.<sup>40–43</sup> Below 1 GPa, the Raman spectrum of  $\gamma$ -IMC is dominated by a hard pressure dependence of the lattice modes contrasting to the analyzed internal modes. However, it is worth noting that the pressure-induced shifts of internal modes in the 1550–1750  $\text{cm}^{-1}$  are large, except for the 1697  $\text{cm}^{-1}$  band. Large frequency shifts are connected to the molecular flexibility, while the behavior of the 1697  $\text{cm}^{-1}$  band indicates strong H-bonding interactions in dimmers responsible for the orientational long-range order of dimmers in chains.

### 1. $\gamma$ crystal $\rightarrow$ $\alpha$ -like crystal transformation

Around 1 GPa, the analysis of the lattice modes reveals a transformation in the long-range order of the  $\gamma$  form. Two additional phonon peaks [localized by an arrow in Fig. 4(a)] are detected and a change in the pressure dependence of the frequency of each mode is clearly observed in Fig. 7 and Table II. The Raman spectrum in the 1550–1750  $\text{cm}^{-1}$  region gives us the opportunity to analyze the molecular conformation of IMC and molecular associations via H bonding. Figure 5(a) indicates that the organization of IMC molecules in dimmers remains unchanged by pressurization up to 3.2 GPa since the 1697  $\text{cm}^{-1}$  band is quasipressure independent. The hard frequency pressure dependence of lattice modes observed between  $P_{\text{atm}}$  and 1 GPa is probably limited by the strong orientational order corresponding to the organization of dimer chains via H bonds. At 3.2 GPa, the detection of a tail on the low-frequency side of the 1697  $\text{cm}^{-1}$  band probably indicates new molecular associations via H bonding between acid and benzoyl groups if the assignment

of  $\nu\text{C}=\text{O}$  stretching vibration determined in the  $\alpha$ -form (Table I) is adopted. The growing of this band to the detriment of the benzoyl  $\nu(\text{C}=\text{O})\text{b-nHb}$  stretching band reveals a concomitant decrease of dimmers, distinctive of the  $\gamma$  form and leading to the coexistence of different molecular conformations, as determined in the  $\alpha$  form.<sup>30</sup> At 4.9 GPa, both the low- and the high-frequency Raman spectra are drastically modified. Both spectra are similar to those of the  $\alpha$  form, with an additional band detected around 1650  $\text{cm}^{-1}$ , only observed in the spectrum of the  $\alpha$  form. In this context, these

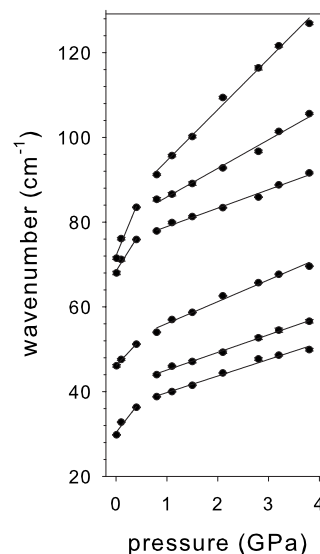


FIG. 7. Pressure induced shifts of the most intense phonon peaks in the  $P_{\text{atm}}$ –4 GPa pressure range. Above 4 GPa, the poor quality of the low-frequency spectrum makes the determination of frequencies impossible.

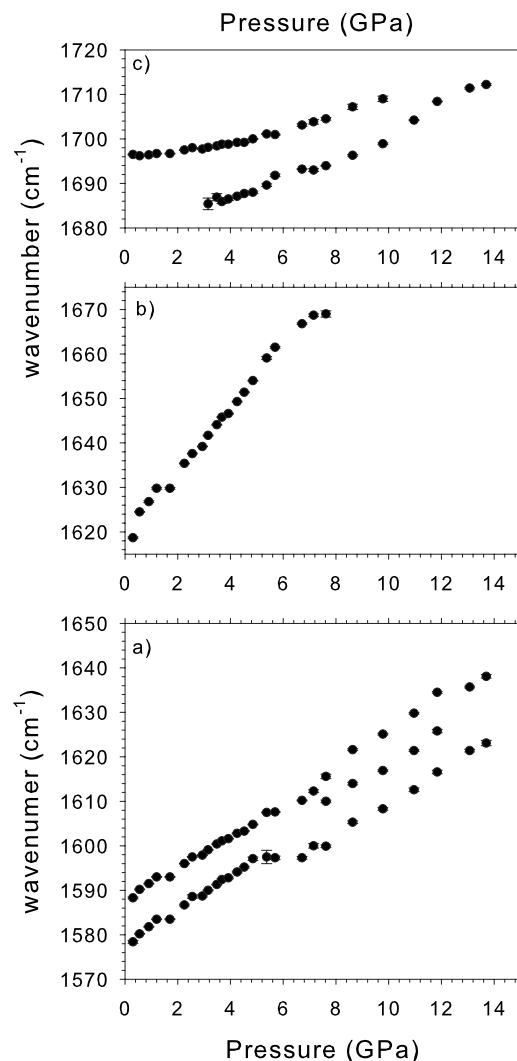


FIG. 8. Pressure induced shifts of internal mode in the 1550–1750  $\text{cm}^{-1}$  for internal band observed under room temperature conditions (a) at 1577 and 1589  $\text{cm}^{-1}$ , (b) at 1616  $\text{cm}^{-1}$ , and (c) at 1697  $\text{cm}^{-1}$ .

modifications of the Raman spectra can be interpreted as a pressure-induced transformation into a metastable state close to the  $\alpha$  form which is denser than the  $\gamma$  form. Both the observations in the low-frequency range and in the 1550–1750  $\text{cm}^{-1}$  region (sharpening of lattice modes and detection of additional external and internal modes) converge into a description of the transformation as an ordering process. The ordering process mainly corresponds to significant modifications in the H-bond network, i.e., to the transformation of the relatively poor packing in dimmers into a more efficient packing in trimmers distinctive of the  $\alpha$  form which has a greater density than the  $\gamma$  form. Consequently, it can be considered that  $\gamma$ -IMC gradually transforms into a crystalline state very close to the  $\alpha$  form by pressurization up to 4.9 GPa. The observation of modifications in the low-frequency spectrum and near 1615  $\text{cm}^{-1}$  at pressures ( $\sim 1$  GPa) well below the observation of changes in the Raman line shape of the 1697  $\text{cm}^{-1}$  band ( $\sim 3.2$  GPa) indicates very strong H bonding distinctive of the  $\gamma$  form since the

TABLE II. Pressure dependence of Raman mode frequencies in the low-frequency range below and above 0.8 GPa and in the high-frequency range below 8 GPa from linear regression.

Mode frequency ( $\text{cm}^{-1}$ )	$\frac{\partial\omega}{\partial P}$ ( $\text{cm}^{-1} \text{ GPa}^{-1}$ )	$\frac{\partial\omega}{\partial P}$ ( $\text{cm}^{-1} \text{ GPa}^{-1}$ )
$P_{\text{atm}}$	$P < 0.8$ GPa	$P > 0.8$ GPa
31	$15.4 \pm 3$	$3.9 \pm 0.2$
46	$12.8 \pm 0.7$	$5.2 \pm 0.3$
67	$19.1 \pm 3$	$4.4 \pm 0.2$
71	$29.2 \pm 5$	$6.8 \pm 0.3$
$P_{\text{atm}}$	$0.8 < P < 8$ GPa	
1577	$3.7 \pm 0.1$	
1588	$3.8 \pm 0.1$	
1616	$6.9 \pm 0.2$	
1697	$0.85 \pm 0.05$	

H-bond network arranged in dimmers remains stable, while lattice modifications and probably conformational changes are observed.

Despite the fact that there is no observation of the  $\gamma$ -to- $\alpha$  transition upon heating IMC, the polymorph of IMC can be compared to that of resorcinol which exhibits  $\alpha$ -crystal to  $\beta$ -crystal transition at 370 K with a volume reduction of about 3%,<sup>44</sup> in which the denser phase ( $\beta$ ) is stable at higher temperatures. The  $\alpha \rightarrow \beta$  phase transition is also observed by pressurization.<sup>14,15</sup> This solid-solid phase transition was described by large rearrangements in the H-bond network accompanied with a weakening of the OH bonds.<sup>45</sup> From the present study and previous structural analyses,<sup>28</sup> it can be considered that  $\gamma$ -IMC, hexagonal ice,<sup>46</sup> and  $\alpha$ -resorcinol<sup>45</sup> have similar structural properties, i.e., an open structure maintained by the directive power of the H bonds. However, depending on the pressurization rate,  $\alpha$  phase of resorcinol transforms into  $\beta$  (slow pressurization) or into a new  $\delta$  phase (rapid pressurization) only observed under pressure. In our experiments carried out on IMC in two different pressure runs, Raman spectra were observed to be similar at comparable pressures, and no additional crystalline phase was detected on compression.

## 2. Crystal $\rightarrow$ amorphous transformation

Above 4.9 GPa, the additional band near 1650  $\text{cm}^{-1}$  clearly disappears, while the other bands are merging into three broad bands. These observations reveal a pressure induced disordering process above 4.9 GPa, probably toward an amorphous state, taking into account the very broad Raman line shape between 1550 and 1750  $\text{cm}^{-1}$  and the disappearance of the lattice modes at 9.8 GPa. The pressure behavior of the Raman band near 1650  $\text{cm}^{-1}$  interpreted as the signature of molecular associations in trimmers distinctive of  $\alpha$ -IMC indicates the rapid breakdown of the H bonded network of the  $\alpha$  phase. Consequently, the number of non-H-bonded IMC molecules increases with pressurization above 4.9 GPa that favors a molecular close packing with a highly

disordered molecular surrounding according to the Raman line shape in the  $1550\text{--}1750\text{ cm}^{-1}$  frequency range. The line shape of the Raman spectrum in the  $1550\text{--}1750\text{ cm}^{-1}$  region composed of three broadbands can be interpreted as resulting from a heterogeneous molecular surrounding. This latter would be produced by several molecular conformations inherent to the very high compression and compatible with a close molecular packing.

PIA was also observed in resorcinol, and more generally, many of materials which exhibit a negative thermal expansion undergo a PIA.<sup>47</sup> It was also observed that PIA in some of the corner-linked framework structures is not observed from the parent phase but from a high-pressure phase.<sup>47</sup> The  $\gamma$  phase of IMC first transforms into a  $\alpha$ -like structure under pressurization prior to amorphize. Several arguments based on high-pressure polymorphism<sup>48</sup> or impeded structural transitions<sup>49</sup> have been proposed to explain the mechanism of PIA. It has also been shown that amorphization and melting of ice were closely linked,<sup>50</sup> and from MD simulations,<sup>51</sup> the structure of the amorphous state of quartz obtained by pressurization was determined to be similar to that of a rapidly quenched thermal glass. By contrast to resorcinol, no additional phase was detected on two different pressure runs carried out on  $\gamma$ -IMC. The structure of the high-pressure amorphous state obtained by rapid or low pressurization appears very similar. Pressure-induced transformations from  $\gamma$ -IMC can be mainly described as transformations in the H-bond network associated with changes in molecular conformation of IMC. The observation of conformational changes in IMC molecules with pressurization, and Raman features observed by pressurization in the  $1550\text{--}1750\text{ cm}^{-1}$  range are interpreted as produced by the collapse of the H-bonded network into a highly disordered and close packing. It has been demonstrated from MD simulations that the collapse of the water molecules into empty interstitial sites was the primary driving force for the PIA leading to a description of the transformation as analogous to mechanical melting.<sup>52</sup> Our results show a close connection between PIA and the mechanism of the H-bonded network collapse which could be consistent to the mechanical melting scenario reported for ice.<sup>3,53</sup>

### B. Analysis of the high density amorphous form

The Raman spectrum in the  $1550\text{--}1750\text{ cm}^{-1}$  region is relatively well defined at 13.7 GPa and can be compared to those of the vitrified state at room temperature and atmospheric pressure by quenching of the liquid state and the liquid at atmospheric pressure and 443 K (Fig. 9). It can be roughly described as composed of three broadened bands, and the line shape of this spectrum appears quite different from that of the vitrified state. It is probably the indication of structural changes in the short-range order with respect to the vitrified state, and then probably a different solid amorphous forms with a very high density. By the release of pressure, the line shape of the Raman spectrum transforms and becomes similar to that of the vitrified state between 7.5 and 4.6 GPa, with a significant shift toward the higher frequencies because of the pressure dependence of the thermal glass.

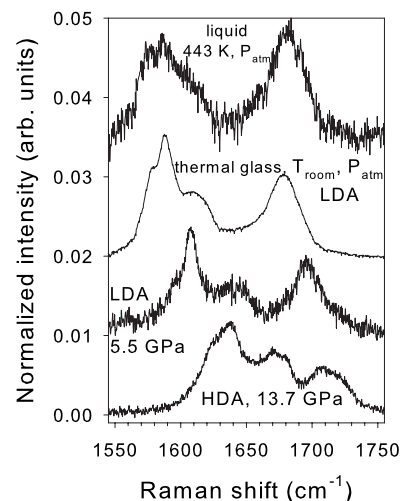


FIG. 9. Raman spectra in the  $1550\text{--}1750\text{ cm}^{-1}$  range of the liquid at 443 K and atmospheric pressure, the thermal glass under room temperature conditions obtained by quench of the liquid, the high-density amorphous state pressurized at 13.7 GPa, and the low-density amorphous state at 5.5 GPa obtained after release of pressure. It is clearly observed that the Raman line shape at 5.5 GPa mimics that recorded after quenching the liquid at room temperature indicating a similar local organization.

This is indicative that the high density amorphous state transforms into a lower density amorphous state which has a local organization similar to that in the vitrified state, as seen in Fig. 9 at 5.5 GPa. The different line shapes of the Raman spectra recorded at 13.7 and 5.5 GPa by depressurization are the signature of two different local organizations characterized by high- and low-density density packings. From Fig. 9, it appears that two different amorphous forms can be produced by two different synthesis routes, i.e., vitrification of the liquid state and PIA of the  $\gamma$  form. By taking into account the number of Raman bands and the Raman line shape in the  $1550\text{--}1750\text{ cm}^{-1}$  region, the degree of disorder in the high-density amorphous state appears to be intermediate between that detected in liquid and in the thermal glass, probably because of the existence of different molecular conformations induced by very high pressurization. The existence of two different solid amorphous forms obtained by different synthesis routes and the ability to be amorphized by pressurization are considered to be two properties for candidate polyamorphic systems.<sup>54</sup>

### V. CONCLUSION

This study reports the description of PIA of  $\gamma$ -IMC toward a high-pressure amorphous state which exhibits between  $1550$  and  $1750\text{ cm}^{-1}$  a Raman line shape clearly different from that of the liquid and the thermal glass (Fig. 9).

The  $\gamma$  phase is characterized by strong and orientational H bonding within dimmers responsible for the poor packing and a lower density than the  $\alpha$  phase, which is stable at higher temperatures. PIA can be described into two successive and contrasting steps. First, above 1 GPa lattice modifications and molecular conformational changes are detected



prior to the breakdown of dimmer chains observed from 3.2 GPa. The H-bonded network distinctive of the  $\gamma$  form collapses into a closer packing induced by new molecular associations distinctive of the  $\alpha$  form, which is detected near 4.9 GPa. The Raman signatures analyzed during pressurization up to 4.9 GPa and corresponding to these structural rearrangements, i.e., the sharpening of lattice modes and the increase of the number of external and internal modes, are characteristic of an ordering process. These results are consistent with a previous study<sup>32</sup> which suggested a PIA and also revealed a pressure-controlled nucleation of the dense  $\alpha$ -crystal form, existing as a stable form under high pressure. In contrast to the first step, the second step of PIA (above 4.9 GPa) appears as a disordering process through the disappearance of Raman bands (lattice modes and the 1615  $\text{cm}^{-1}$  band) and the merging of internal bands between 1550 and 1750  $\text{cm}^{-1}$  in three broadbands. This second step of amorphization corresponds to the breakdown of the H-bonded network distinctive of the  $\alpha$  form, and PIA can be globally described from atmospheric pressure as a gradual collapse transformation of the H-bonded network into a disordered high-pressure state. The same kind of PIA connected to the collapse of H-bonded structure has been observed on other materials which exhibit negative thermal expansion upon heating.<sup>3,14,15,47</sup> This original property is similar to the situation of metastability of the dense  $\alpha$  phase with respect to the  $\gamma$  form, and so can be suspected to be involved in the underlying mechanism of pressure-induced disordering.

The Raman line shape of the high-pressure amorphous state transforms upon decompression toward that of the ther-

mal glass near 5.5 GPa (Figs. 6 and 9), suggesting a HDA  $\rightarrow$  LDA transition. Such a transformation could correspond to a polyamorphic transition, as observed in ice,<sup>3,53</sup> but not yet evidenced in organic molecular compounds.

By further depressurization of the low-density amorphous state, dimmer chains distinctive of  $\gamma$ -IMC are directly formed indicating the direct formation of the poor packing structure upon decompression rather than the dense  $\alpha$  phase. The preferential formation of H-bonded dimmer chains as long-range order indicates that the route to the high-pressure disordered state is not reversible.

This study clearly reveals first the capability of  $\gamma$ -IMC to be amorphized by compression, and second, that two structurally different amorphous forms can be produced by two different synthesis routes. The crystal-to-crystal transformation observed upon compression and described as the collapse of the H-bonded network can be considered as corresponding to a density-driven transition. Consequently, the transformation of the Raman spectra upon decompression between 13.7 and 5.5 GPa (Fig. 9) could provide the indication that a density-driven transformation, i.e., a polyamorphic transformation, might occur within solid amorphous indomethacin similar to the LDA-HDA transformation in ice.<sup>2</sup> Moreover, the common originalities between the polymorphisms of IMC and ice, related to the low packing of the H-bonded network in the more stable crystalline state, are an additional indication, suggesting that indomethacin can be classified among the candidate polyamorphic systems.<sup>54</sup>

<sup>1</sup>L. Bosio, G. P. Johari, and J. Teixeira, Phys. Rev. Lett. **56**, 460 (1986).

<sup>2</sup>O. Mishima, L. D. Calvert, and E. Whalley, Nature (London) **314**, 76 (1985).

<sup>3</sup>O. Mishima, L. D. Calvert, and E. Whalley, Nature (London) **310**, 393 (1984).

<sup>4</sup>I. Saika-Voivod, F. Sciortino, and P. H. Poole, Phys. Rev. E **63**, 011202 (2000).

<sup>5</sup>C. A. Angell, R. D. Bressel, M. Hemmati, E. J. Sare, and J. C. Tucker, Phys. Chem. Chem. Phys. **2**, 1559 (2000).

<sup>6</sup>S. Sampath, C. J. Benmore, K. M. Lantzky, J. Neufeind, K. Leinenweber, D. L. Price, and J. L. Yarger, Phys. Rev. Lett. **90**, 115502 (2003).

<sup>7</sup>M. Guthrie, C. A. Tulk, C. J. Benmore, J. Xu, J. L. Yarger, D. D. Klug, J. S. Tse, H.-K. Mao, and R. J. Hemley, Phys. Rev. Lett. **93**, 115502 (2004).

<sup>8</sup>G. Monaco, S. Falconi, W. A. Crichton, and M. Mezouar, Phys. Rev. Lett. **90**, 255701 (2003).

<sup>9</sup>W. A. Crichton and N. L. Ross, Miner. Mag. **69**, 273 (2005).

<sup>10</sup>S. Stolen, T. Grande, and H. B. Johnsen, Phys. Chem. Chem. Phys. **4**, 3396 (2002).

<sup>11</sup>S. Ekbundit, K. Leinenweber, J. L. Yarger, J. S. Robinson, V. M. Verhelst, and G. H. Wolf, J. Solid State Chem. **126**, 300 (1996).

<sup>12</sup>N. Chandrabhas, A. K. Sood, D. V. S. Muthu, C. S. Sundar, A. Bharathi, Y. Hariharan, and C. N. R. Rao, Phys. Rev. Lett. **73**, 3411 (1994).

<sup>13</sup>M. P. Pasternak, R. D. Taylor, M. B. Kruger, R. Jeanloz, J. P. Itie, and A. Polian, Phys. Rev. Lett. **72**, 2733 (1994).

<sup>14</sup>S. K. Deb, M. A. Rekha, A. P. Roy, V. Vijayakumar, S. Meenakshi, and B. K. Godwal, Phys. Rev. B **47**, 11491 (1993).

<sup>15</sup>R. Rao, T. Sakuntala, and B. K. Godwal, Phys. Rev. B **65**, 054108 (2002).

<sup>16</sup>R. Rao, T. Sakuntala, A. K. Arora, and S. K. Deb, J. Chem. Phys. **121**, 7320 (2004).

<sup>17</sup>S. M. Sharma and S. K. Sikka, Prog. Mater. Sci. **40**, 1 (1996).

<sup>18</sup>A. Ha, I. Cohen, X. Zhao, M. Lee, and D. Kivelson, J. Phys. Chem. **100**, 1 (1996).

<sup>19</sup>G. P. Johari and C. Ferrari, J. Phys. Chem. B **101**, 10191 (1997).

<sup>20</sup>A. Hedoux, Y. Guinet, and M. Descamps, Phys. Rev. B **58**, 31 (1998).

<sup>21</sup>A. Hedoux, O. Hernandez, J. Lefebvre, Y. Guinet, and M. Descamps, Phys. Rev. B **60**, 9390 (1999).

<sup>22</sup>A. Hedoux, P. Derollez, Y. Guinet, A. J. Dianoux, and M. Descamps, Phys. Rev. B **63**, 144202 (2001).

<sup>23</sup>A. Hedoux, Y. Guinet, and M. Descamps, J. Raman Spectrosc. **32**, 677 (2001).

<sup>24</sup>A. Hedoux, Y. Guinet, M. Foulon, and M. Descamps, J. Chem. Phys. **116**, 9374 (2002).

<sup>25</sup>H. Tanaka, R. Kurita, and H. Mataka, Phys. Rev. Lett. **92**, 025701 (2004).

<sup>26</sup>V. Andronis and G. Zografi, J. Non-Cryst. Solids **271**, 236 (2000).

- <sup>27</sup>K. J. Crowley and G. Zografi, *J. Pharm. Sci.* **91**, 492 (2002).
- <sup>28</sup>T. J. Kistenmacher and R. E. Marsh, *J. Am. Chem. Soc.* **94**, 1340 (1972).
- <sup>29</sup>N. Kaneniwa, M. Otsuka, and T. Hayashi, *Chem. Pharm. Bull. (Tokyo)* **33**, 3447 (1985).
- <sup>30</sup>X. Chen, K. R. Morris, U. J. Griesser, S. R. Byrn, and J. G. Stowell, *J. Am. Chem. Soc.* **124**, 15012 (2002).
- <sup>31</sup>L. Borka, *Acta Pharm. Suec* **11**, 295 (1974).
- <sup>32</sup>T. Okumura, M. Ishida, K. Takayama, and M. Otsuka, *J. Pharm. Sci.* **95**, 689 (2006).
- <sup>33</sup>T. Wu and L. Yu, *J. Phys. Chem. B* **110**, 15694 (2006).
- <sup>34</sup>L. S. Taylor and G. Zografi, *Pharm. Res.* **14**, 1691 (1997).
- <sup>35</sup>A. G. Schmidt, S. Wartewig, and K. M. Picker, *J. Raman Spectrosc.* **35**, 360 (2004).
- <sup>36</sup>H. K. Mao, J. Xu, and P. M. Bell, *J. Geophys. Res.* **91**, 4673 (1986).
- <sup>37</sup>L. S. Taylor and G. Zografi, *Pharm. Res.* **15**, 755 (1998).
- <sup>38</sup>T. Matsumoto and G. Zografi, *Pharm. Res.* **16**, 1722 (1999).
- <sup>39</sup>T. Watanabe, N. Wakiyama, F. Usui, M. Ikeda, T. Isobe, and M. Senna, *Int. J. Pharm.* **226**, 81 (2001).
- <sup>40</sup>R. Zallen, *Phys. Rev. B* **9**, 4485 (1974).
- <sup>41</sup>R. Zallen and M. L. Slade, *Phys. Rev. B* **18**, 5775 (1978).
- <sup>42</sup>A. Hedoux, Y. Guinet, F. Capet, F. Affouard, and M. Descamps, *J. Phys.: Condens. Matter* **14**, 8725 (2002).
- <sup>43</sup>A. Hedoux, Y. Guinet, P. Derollez, J. F. Willart, F. Capet, and M. Descamps, *J. Phys.: Condens. Matter* **15**, 8647 (2003).
- <sup>44</sup>Y. Ebisuzaki, L. H. Askari, A. M. Bryan, and M. F. Nicol, *J. Chem. Phys.* **87**, 6659 (1987).
- <sup>45</sup>G. E. Bacon and E. J. Lisher, *Acta Crystallogr., Sect. B: Struct. Crystallogr. Cryst. Chem.* **B36**, 1908 (1980).
- <sup>46</sup>V. F. Petrenko and R. W. Whitworth, *Physics of Ice* (Oxford University Press, Oxford, 1999).
- <sup>47</sup>S. K. Sikka, *J. Phys.: Condens. Matter* **16**, S1033 (2004).
- <sup>48</sup>D. M. Teter, R. J. Hemley, G. Kresse, and J. Hafner, *Phys. Rev. Lett.* **80**, 2145 (1998).
- <sup>49</sup>P. Gillet, J. Badro, B. Varrel, and P. F. McMillan, *Phys. Rev. B* **51**, 11262 (1995).
- <sup>50</sup>O. Mishima, *Nature (London)* **384**, 546 (1996).
- <sup>51</sup>J. Badro, P. Gillet, and J.-L. Barrat, *Europhys. Lett.* **42**, 643 (1998).
- <sup>52</sup>J. S. Tse, *J. Chem. Phys.* **96**, 5482 (1992).
- <sup>53</sup>O. Mishima and H. E. Stanley, *Nature (London)* **396**, 329 (1998).
- <sup>54</sup>M. C. Wilding, M. Wilson, and P. F. McMillan, *Chem. Soc. Rev.* **35**, 964 (2006).